Available online at www.sciencedirect.com
SCIENCE DIRECT®
Journal of Organometallic Chemistry 691 (2006) 2846–2852
Journal of Organometallic Chemistry
www.elsevier.com/locate/jorganchem

Synthesis of platinum-iodo-alkyl/aryl complexes in ligand-exchange reactions: Determination of the structure of Pt{(*S*,*S*)-bdpp}(X)I complexes (X = Me, I) by X-ray crystallography

László Jánosi [a], László Kollár [a,b,*], Piero Macchi [c], Angelo Sironi [c,*]

[a] *University of Pécs, Department of Inorganic Chemistry, H-7624 Pécs, Ifjúság, P. O. Box 266, Hungary*
[b] *Research Group for Chemical Sensors of the Hungarian Academy of Sciences, H-7624 Pécs, P.O. Box 266, Hungary*
[c] *Dipartimento di Chimica Strutturale e Stereochimica Inorganica dell'Università di Milano, Via G. Venezian 21, 20133 Milano, Italy*

Received 27 October 2005; received in revised form 16 February 2006; accepted 20 February 2006
Available online 28 February 2006

Abstract

Pt{(*S*,*S*)-bdpp}(R)I (bdpp = 2,4-bis(diphenylphosphino)pentane; R = Me, Ph, Bz, 2-Tioph) complexes were formed in alkyl/aryl ligand – iodide ligand-exchange reactions by reacting the corresponding Pt{(*S*,*S*)-bdpp}R_2 complexes with methyl iodide. The Pt{(*S*,*S*)-bdpp}(Me)I complex was isolated and fully characterised. The influence of the X ligand on the platinum-bdpp chelate conformation was investigated in Pt{(*S*,*S*)-bdpp}(X)I (X = I, $SnCl_3$, Me) complex series by means of X-ray crystallography.

Keywords: Platinum; Iodo-complex; X-ray crystallography; Chelate

1. Introduction

The reactivity of the platinum–alkyl bond towards insertion reactions has been the aim of investigations for a long time due to its importance in homogeneous catalytic reactions [1]. Among the elementary steps, the insertion of carbon monoxide into the platinum–alkyl bond of a Pt(diphosphine)(alkyl)X (X = halide, $SnCl_3$) complex is a crucial one in platinum catalysed hydroformylation [2]. The insertion of CO into Pt–carbon bonds has been extensively studied both in case of Pt–alkyl and aryl complexes containing monodentate phosphine ligands [3]. Although detailed mechanistic investigations shed some light on the formation of Pt–acyl complexes from Pt–alkyl complexes containing diphosphines [4], less are known about the mechanistic details of the formation of the Pt–alkyl intermediate itself. The importance of this step is due to its determining role in the stereochemical outcome of the reaction, i.e., platinum-chelate conformation might have a great impact on the stereochemistry of the alkene insertion. Moreover, sporadic results are available on the change of the platinum-chelate conformation by varying the diphosphine ligands with catalytic importance [5].

Due to their high catalytic importance, the synthesis and structural investigation of Pt(diphosphine)(R)X complexes is still of direct interest. Prompted by the successful isolation and structural characterisation of Pt(bdpp)I($SnCl_3$) [6], we decided to provide a novel methodology for the synthesis of its Pt(bdpp)I(alkyl/aryl) analogues containing this chiral diphosphine, which is favourably used in various asymmetric homogeneous catalytic reactions. A new methodology including the application of methyl iodide (and further iodo-alkenes) has been developed for their synthesis. Furthermore, the structural characterisation of the above complexes, that could be the key intermediates in various homogeneous catalytic reactions, might shed some light on the control of the stereochemistry in enantioselective homogeneous reactions.

* Corresponding authors. Tel.: +36 72 327622/4153; fax: +36 72 501527 (L. Kollár).
E-mail address: kollar@ttk.pte.hu (L. Kollár).

0022-328X/$ - see front matter © 2006 Elsevier B.V. All rights reserved.
doi:10.1016/j.jorganchem.2006.02.026

2. Results and discussion

2.1. Synthesis and NMR characterization of Pt{(S,S)-bdpp}(R)I and Pt{(S,S)-bdpp}R_2 complexes

The synthesis of Pt(diphosphine)(Me)X (X = halide) is a straightforward one. From the many possibilities, the alkylation of Pt(diene)X_2 with tetramethyltin followed by the substitution with the corresponding diphosphine is dominating. A further methodology implies the alkyl/halide ligand-exchange reactions between Pt(diphosphine)X_2 and Pt(diphosphine)R_2 (R = alkyl) [7].

The diary/dialkyl complexes Pt(1,5-COD)R_2 (R = Me (**1a**); Ph (**1b**); Bz (**1c**); 2-Tioph (**1d**)), served as starting materials to ligand exchange investigations, have been synthesised from Pt(1,5-COD)Cl_2 (**1**) [8]. The substitution of the diene with (*S*,*S*)-bdpp resulted in the formation of the corresponding Pt{(*S*,*S*)-bdpp}R_2 (**2a**–**2d**) complexes in excellent yields (Scheme 1).

Since the preliminary experiments with **2a** have shown the undesired side reaction of chloride-methyl ligand-exchange in chloroform (resulting in the formation of Pt(bdpp)Cl_2 and Pt(bdpp)(Me)Cl)) the further reactions have been carried out in acetonitril.

By reacting **2a** with MeI the exclusive formation of **3a** has been observed in a complete reaction within 2 h. The clean reaction provided **3a** as a yellow crystalline material. The substitution of the 'second' methyl ligand for iodide was failed even in case of 10 molar equivalents of MeI. Similar behaviour has been observed when *n*-octyl-iodide has been used as 'iodide-source'. However, both methyl ligands have been substituted by iodo ligands when CH_2I_2 was used. The starting complex **2a** has been converted completely to Pt(bdpp)I_2 (**4**) [6] which has been isolated as a pale yellow crystalline material. No reaction occurred in the presence of iodobenzene.

The two diaryl-platinum derivatives, **2b** and **2d** behaved similarly to **2a**, i.e., monoiodo complexes **3b** and **3d** were formed by using MeI. However, the reaction was not complete and the isolation of these two products in high purity failed. (**3b** and **3d** have been synthesised and isolated by using independent reaction pathways (see Section 3).) In the reaction of **2b** (or **2d**) with CH_2I_2 (**4**) was obtained as major product.

Surprisingly, the reaction of the dibenzyl derivative, **2c** with MeI resulted in a more complicated reaction mixture (Scheme 2). In addition to the expected benzyl-iodo derivative **3c** and diiodo complex **4**, a further monoiodo complex, Pt(bdpp)(Me)I was formed due to the benzyl–methyl ligand exchange. The reaction of **2c** with CH_2I_2 resulted in the formation of **4** (major product), **3c** and Pt(bdpp)(CH_2)I (**3e**) (Scheme 3). It has to be noted that the formation of an additional complex showing a pair of doublets in ^{31}P NMR has been observed as well, which can be assigned to a methylene bridging compound [{Pt(bdpp)I}$_2$(η^1,η^1-CH_2)] (**5**) (vide infra).

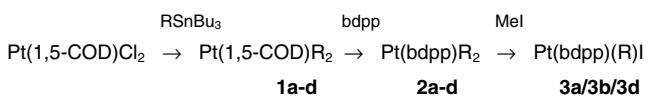

Scheme 1. The formation of platinum-iodo-alkyl/aryl complexes in the reaction of platinum-dialkyl/diaryl complexes with methyl iodide (R = Me (a); Ph (b); Bz (c); 2-Tioph (d)).

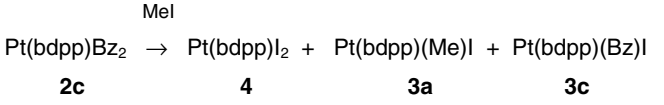

Scheme 2. The reaction of platinum-dibenzyl complex **2c** with methyl iodide.

The dialkyl/diaryl complexes **2a**–**2d** showing a single central line (flanked by platinum satellites) can be easily identified by ^{31}P NMR spectroscopy (Table 1). The typical $^1J(^{195}Pt,^{31}P)$ coupling constants of diagnostic value falling in the range of 1700–2000 Hz show the strong *trans* influence of the alkyl/aryl group.

The ^{31}P NMR measurements of platinum complexes **3a**–**3e** provided a sensitive probe for complex structures. The magnitude of the one-bond interactions, i.e., $^1J(^{195}Pt,^{31}P)$ coupling constants have been shown to depend strongly on whether the phosphorus has an aryl/alkyl or iodo ligand in *trans* position. The phosphorus *trans* to iodo ligand possesses $^1J(^{195}Pt,^{31}P)$ coupling constants larger than 3500 Hz. However, the phosphorus nuclei *trans* to alkyl/aryl substituent have the typical platinum–phosphorus coupling of 1600–2000 Hz similar to those observed in case of dialkyl/diaryl complexes **2a**–**2d**.

2.2. Structural characterization of *3a* and *4* by X-ray diffraction

The crystal structures of **3a** and **4** share the feature of having $Z' > 1$ (2 and 3, respectively). In the crystals of **3a** there are two independent [Pt{(*S*,*S*)-bdpp}(Me)I] molecules in the asymmetric unit (**3a**-1 and **3a**-2) while the crystals of **4** are built from the packing of [Pt{(*S*,*S*)-bdpp}I_2], CH_2I_2 and MeCN molecules, in the 3:1:1 ratio; the three independent [Pt{(*S*,*S*)-bdpp}I_2], molecules being labelled **4**-1, **4**-2 and **4**-3. In both cases we do not observe anomalous van der Waals contacts. Fig. 2 report the ORTEP [9] drawings of the five independent conformers in their absolute configuration. Relevant bond parameters are reported in Tables 2 and 3.

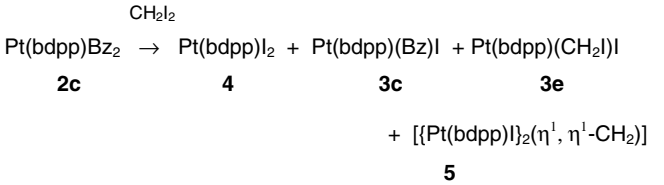

Scheme 3. The reaction of platinum-dibenzyl complex **2c** with methylene iodide.

Table 1
^{31}P NMR data of the platinum–bdpp complexes[a]

Complexes	δP_A[b] (ppm)	δP_B[b] (ppm)	$^1J(^{195}Pt,^{31}P_A)$ (Hz)	$^1J(^{195}Pt,^{31}P_B)$ (Hz)	$^2J(P_A,P_B)$ (Hz)
$Pt(CH_3)_2$(bdpp) (**2a**)	16.4	–	1784	–	–
$Pt(Ph)_2$(bdpp) (**2b**)	13.7	–	1686	–	–
$Pt(Bz)_2$(bdpp) (**2c**)	16.7	–	1873	–	–
$Pt(2\text{-Tioph})_2$(bdpp) (**2d**)	13.0	–	1973	–	–
$PtI(CH_3)$(bdpp) (**3a**)	11.2	8.5	1700	4005	23
PtI(Ph)(bdpp) (**3b**)	8.2	7.9	1630	3903	23
PtI(Bz)(bdpp) (**3c**)	9.4	15.3	1655	4176	25
PtI(2-Tioph)(bdpp) (**3d**)	9.5	8.5	1916	3627	24
$PtI(CH_2I)$(bdpp) (**3e**)	14.7	16.3	1612	4285	26
PtI_2(bdpp) (**4**)	–	5.8	–	3252	–
$[\{Pt(bdpp)I\}_2(\eta^1,\eta^1\text{-}CH_2)]$ (**5**)	7.0	8.4	ca. 2826[e]	ca. 3835[e]	20
$PtI(SnCl_3)$(bdpp)[f]	10.6[c]	5.4[d]	2786	3278	24

[a] Spectra were measured in acetonitrile with D_2O insert (at room temperature).
[b] P_A *trans* to aryl/alkyl ligand, P_B *trans* to I.
[c] $^2J_{trans}$ (^{31}P,^{117}Sn) = 3937 Hz, $^2J_{trans}$ (^{31}P,^{119}Sn) = 4105 Hz.
[d] $^2J_{cis}$(^{31}P,$^{117/119}$Sn) = 157 Hz (^{117}Sn and ^{119}Sn *cis*-satellites coincide).
[e] The uncertainty in the determination of the coupling constants is due to the overlapping satellites with the central lines of other species (**3c**, **3e**, **4**).
[f] See Ref. [6].

Table 2
Selected bond lengths (Å) distances and angles (°) for **4**

	Mol. A (N = 1, X = 1, Y = 2)	Mol. B (N = 2, X = 3, Y = 4)	Mol. C (N = 3, X = 5, Y = 6)
Pt(N)–P(X)	2.263(2)	2.250(2)	2.247(2)
Pt(N)–P(Y)	2.237(2)	2.253(2)	2.246(2)
Pt(N)–I(X)	2.652(1)	2.645(1)	2.638(1)
Pt(N)–I(Y)	2.630(1)	2.670(1)	2.649(1)
P(X)–C(X11)	1.804(7)	1.824(6)	1.832(7)
P(X)–C(X21)	1.809(6)	1.822(6)	1.818(7)
P(X)–C(N1)	1.863(6)	1.851(6)	1.854(8)
P(Y)–C(Y11)	1.811(6)	1.819(6)	1.812(6)
P(Y)–C(Y21)	1.825(6)	1.816(6)	1.836(7)
P(Y)–C(N3)	1.845(6)	1.851(7)	1.825(6)
C(N1)–C(N2)	1.518(10)	1.530(10)	1.499(12)
C(N1)–C(N4)	1.551(10)	1.531(11)	1.512(13)
C(N2)–C(N3)	1.511(11)	1.514(10)	1.567(11)
C(N3)–C(N5)	1.514(11)	1.514(11)	1.522(10)
P(X)–Pt(N)–P(Y)	95.96(4)	91.86(4)	92.58(5)
I(X)–Pt(N)–I(Y)	87.07(4)	88.06(4)	88.63(5)
P(X)–Pt(N)–I(Y)	169.88(4)	173.36(4)	174.67(5)
P(Y)–Pt(N)–I(X)	175.47 (4)	171.11(5)	173.40(5)
Pt(N)–P(X)–C(X11)–C(X12,6)	155.2(6)	116.5(6)	116.2(6)
Pt(N)–P(X)–C(X21)–C(X22,6)	72.2(6)	154.2(6)	178.7(6)
Pt(N)–P(Y)–C(Y11)–C(Y12,6)	53.2(6)	14.6(6)	3.1(6)
Pt(N)–P(Y)–C(Y21)–C(Y22,6)	16.7(6)	111.5(6)	119.5(6)
Pt(N)–P(X)–C(N1)–C(N2)	−20.5(7)	−72.2(5)	−68.3(6)
P(X)–C(N1)–C(N2)–C(N3)	56.9(9)	24.3(8)	35.4(9)
C(N1)–C(N2)–C(N3)–P(Y)	−82.1(8)	44.9(8)	34.1(9)
C(N2)–C(N3)–P(Y)–Pt(N)	65.1(6)	−61.3(5)	−66.9(5)
C(N3)–P(Y)–Pt(N)–P(X)	−29.1(3)	11.2(3)	27.3(3)
P(Y)–Pt(N)–P(X)–C(N1)	10.6(3)	42.2(2)	28.1(3)
Pt(N)–P(X)–C(N1)–C(N4)	−148.9(4)	158.0(5)	163.9(7)
Pt(N)–P(Y)–C(N3)–C(N5)	−62.9(6)	169.1(5)	167.0(5)

The coordination around the Pt atoms of both [Pt{(*S*,*S*)-bdpp}IMe] and [Pt{(*S*,*S*)-bdpp}I_2], see Fig. 1, is square planar with a slight tetrahedral distortion: one P atom and its *trans* counterpart (C or, I) being slightly displaced above the Pt coordination plane while the other P atom (and its *trans* counterpart) are slightly displaced below. This feature can also be monitored by the values of the *trans* X–Pt–Y angles which significantly differ from 180° (Tables 2 and 3).

All bond distances fall in the usual range and the only significant, but expected, intra-molecular effect is the lengthening of the Pt–P bond *trans* to the Pt–Me one in **3a**. This is also associated to a marginal shortening of the Pt–P bond *trans* to the Pt–I one (which average 2.223 Å

Table 3
Selected bond lengths (Å) distances and angles (°) for **3a**

	Mol. A (N = 1, X = 1, Y = 2)	Mol. B (N = 2, X = 3, Y = 4)
Pt(N)–P(X)	2.217(1)	2.230(1)
Pt(N)–P(Y)	2.323(1)	2.316(1)
Pt(N)–I(N)	2.6706(4)	2.6730(5)
Pt(N)–C(N)	2.222(4)	2.292(4)
P(X)–C(X11)	1.821(5)	1.823(5)
P(X)–C(X21)	1.816(5)	1.831(5)
P(X)–C(N1)	1.856(6)	1.863(4)
P(Y)–C(Y11)	1.819(4)	1.822(5)
P(Y)–C(Y21)	1.838(5)	1.827(4)
P(Y)–C(N3)	1.867(4)	1.842(4)
C(N1)–C(N2)	1.547(7)	1.533(6)
C(N1)–C(N4)	1.520(8)	1.552(7)
C(N2)–C(N3)	1.541(6)	1.544(7)
C(N3)–C(N5)	1.537(7)	1.534(7)
P(X)–Pt(N)–P(Y)	95.98(4)	91.65(4)
C(N)–Pt(N)–I(N)	85.91(9)	84.0(1)
P(X)–Pt(N)–I(N)	174.04(4)	172.4(1)
P(Y)–Pt(N)–C(N)	171.37(4)	172.2(1)
Pt(N)–P(X)–C(X11)–C(X12,6)	13.7(4)	124.8(4)
Pt(N)–P(X)–C(X21)–C(X22,6)	51.6(4)	148.5(4)
Pt(N)–P(Y)–C(Y11)–C(Y12,6)	78.1(4)	17.3(4)
Pt(N)–P(Y)–C(Y21)–C(Y22,6)	154.3(4)	106.2(4)
Pt(N)–P(X)–C(N1)–C(N2)	65.2(4)	−74.7(3)
P(X)–C(N1)–C(N2)–C(N3)	−83.2(4)	24.3(5)
C(N1)–C(N2)–C(N3)–P(Y)	59.1(5)	46.1(5)
C(N2)–C(N3)–P(Y)–Pt(N)	−21.8(4)	−61.1(3)
C(N3)–P(Y)–Pt(N)–P(X)	10.3(2)	10.3(1)
P(Y)–Pt(N)–P(X)–C(N1)	−28.9(2)	44.3(2)
Pt(N)–P(X)–C(N1)–C(N4)	−64.0(4)	156.4(3)
Pt(N)–P(Y)–C(N3)–C(N5)	−151.7(3)	170.7(3)

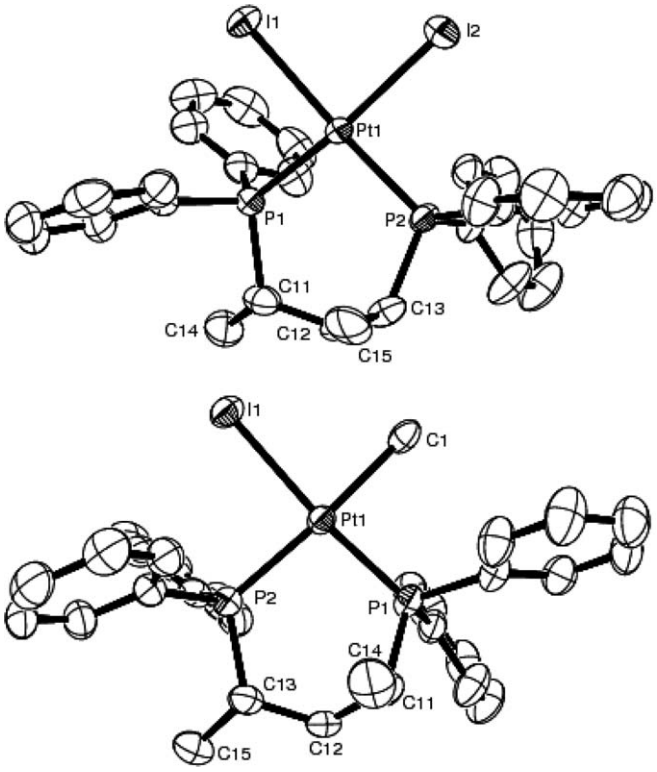

Fig. 1. ORTEP3 drawings of representative molecules of [Pt{(*S*,*S*)-bdpp}I_2] (top) and [Pt{(*S*,*S*)-bdpp}(Me)I] (bottom). The view is down to the Pt 'square planar' coordination plane. Thermal ellipsoids were drawn at the 50% probability level. Hydrogen atoms were omitted for clarity.

in **3a** while the average of the six independent Pt–I in **4** is 2.249 Å).

The major stereochemical effects highlighted by this study concern the shape variability of the bdpp ligand. Indeed, this ligand, even when bounded to a metal, can assume many different conformations which, due to the presence of bulky ring substituents (the phenyls), have largely different shapes. Thus, we may suppose the presence in solution of many 'different' building blocks which should favour the occurrence of phenomena like conformational polymorphism and/or the presence of more than one independent molecule in the asymmetric unit. Actually we may recognise in the two crystal structures three different building blocks (**A**, **B** and **C**) namely: **A** with an envelope conformation of the metallacycle and one axial, one equatorial and two bisectional phenyls (molecules **4**-1 and **3a**-1, which are related by a two-fold rotation about the P–Pt–P bisector); **B** with a boat/twist-boat conformation, one bisectional, one equatorial and two axial phenyls (molecules **4**-2 and **3a**-2); and **C** with delta skew-boat conformation, two equatorial and two axial phenyls (molecule **4**-3) (Fig. 2).

As previously observed in the Pt(bdpp)I($SnCl_3$) crystals [6] when the metallacycle conformation changes substantially, like in the **A**/**C** interconversion, there are correspondingly large variations in the axial/equatorial character and in the face/edge exposure of the phenyl rings. The bond angles at the Pt atom are also sensitive to the conformation of the BDPP ligand since the conformations with an axial methyl group (envelope, twist-chair, chair) require a larger P–Pt–P 'bite' angle [95.96(4)° and 95.98(4) in molecules **4**-1 and **3a**-1, respectively] than the conformations with two equatorial methyls (those close to δ-skew) [92.58(5)° in **4**-3 and 91.86(4)° and 91.65(4) in molecules **4**-2 and **3a**-2, respectively] [9].

In Fig. 3 we report three further conformations (**D**–**F**) of bdpp observed in the known crystal phases of square planar complexes [M{(*S*,*S*)-bdpp}L_2]. From the data in Tables 2 and 3 and a glance on **A**–**F** conformers, it is clear that (i) six-membered metallacycles are rather flexible; (ii) even if, according to experimental and theoretical data [10], the skew conformations should be slightly preferred, the tendency of methyl groups to occupy equatorial positions can be easily violated; (iii) large variations of the ring conformations do affect the P–M–P angle hence, particularly in the presence of large substituents, the overall metal stereochemistry; (iv) the orientation of the phenyl substituents is not strictly affected by the metallacycle conformation.

According to the structure correlation method [10], the variability of the metallacycle stereochemistry observed in the solid state should imply a fast solution dynamics. On

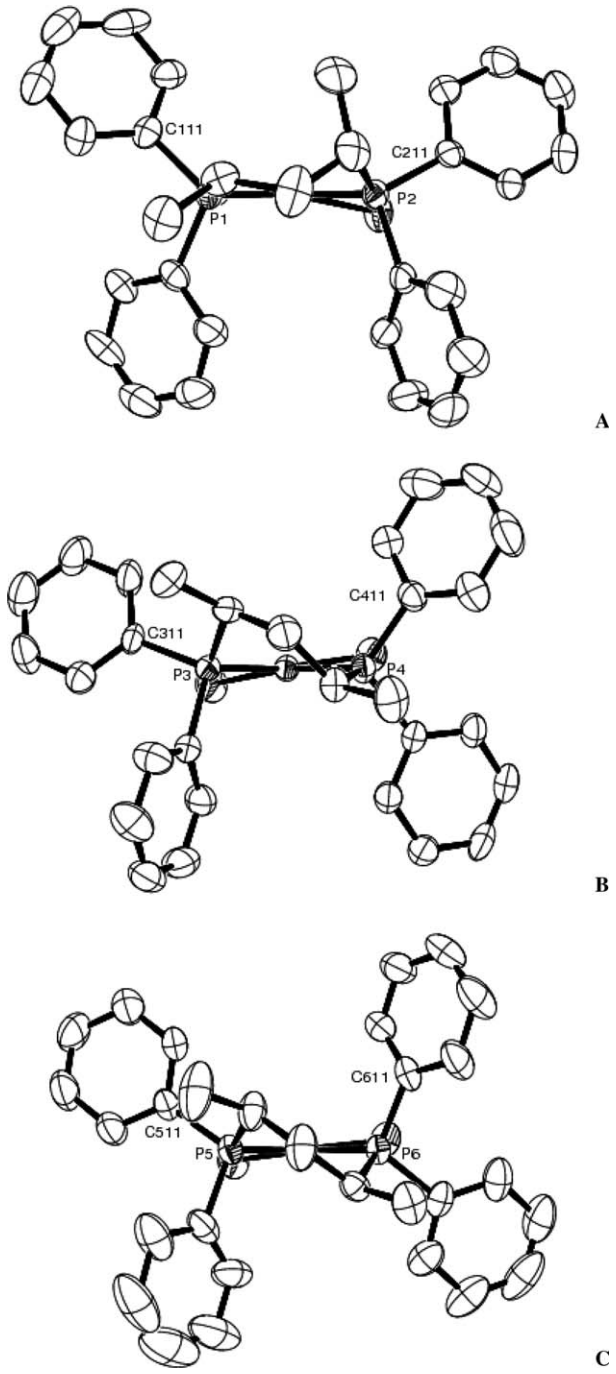

Fig. 2. ORTEP3 drawings of different metallacycle conformers, view along the P–Pt–P bisector, found in the crystal phases [Pt{(*S*,*S*)-bdpp}I_2]·MeCN·CH_2I_2 (**4**) and [Pt{(*S*,*S*)-bdpp}(Me)I] (**3a**). (A) molecule(s) **4**-1 (representative also of **3a**-1); (B) molecule(s) **4**-2 (representative also of **3a**-2); (C) molecule **4**-3. Thermal ellipsoids were drawn at the 50% probability level. Hydrogen atoms were omitted for clarity.

the other hand, the dynamically averaged molecular configurations of [M{(*S*,*S*)-bdpp}L_2] and [M{(*R*,*R*)-bdpp}L_2] must be enantiomeric. Thus, although flexible, this chiral ancillary ligand is anyway able to control the stereochemistry of the alkene insertion but its role is not easily recognizable from just a single structural investigation.

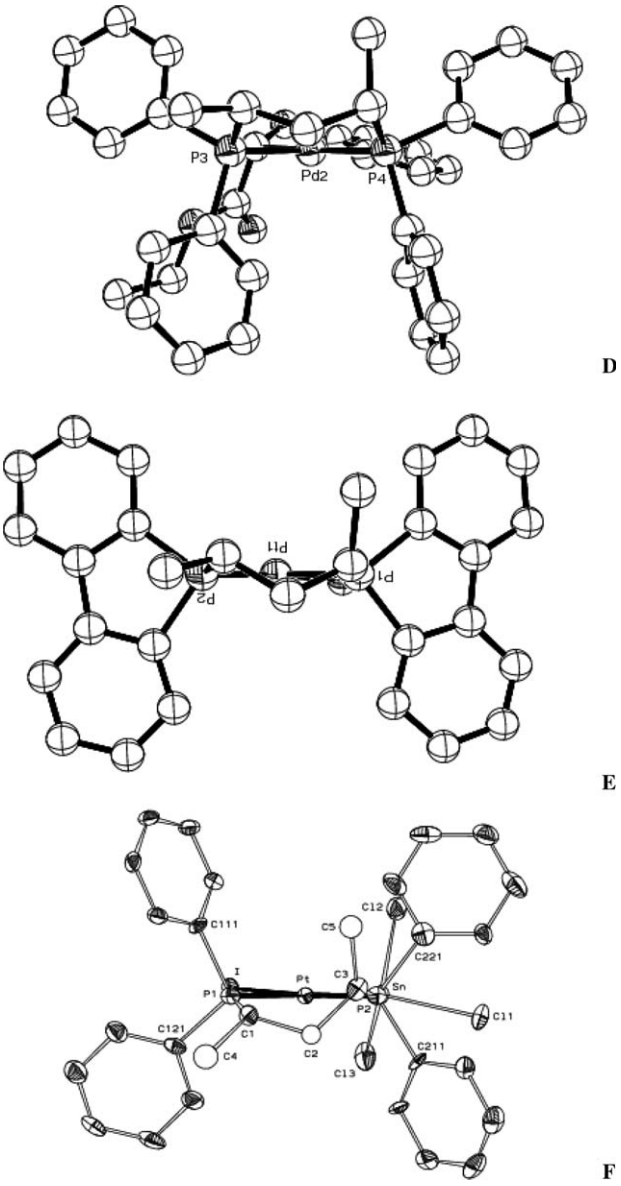

Fig. 3. ORTEP3 drawings of different metallacycle conformers, view along the P–Pt–P bisector, found in the known crystal phases of square planar complexes [M{(*S*,*S*)-bdpp}L_2]. (D) [Pd(bdpp)((R)-(Ethoxycarbonylmethineoxy-1,2-phenylene))]; [14] (E) [Pt(pentane-2,4-diyl-bis(5H-dibenzo-phosphoindole))Cl_2)]; [15] (F) [Pt(bdpp)I($SnCl_3$)] [6] highlighting the flexibility of the bdpp ligand.

3. Experimental

3.1. General

The Pt(1,5-COD)Cl_2 and Pt(1,5-COD)$(Me)_2$ complexes as well as tin-derivatives (phenyl-tributyltin, 2-tiophenyl-tributyltin) were purchased from Aldrich. (*S*,*S*)-bdpp was purchased from Strem. Diarylated complexes (**1b** and **1d**) were prepared according to a known procedure by reacting Pt(1,5-COD)Cl_2 with $PhSnBu_3$ and (2-Tioph)$SnBu_3$, respectively [7]. The dibenzyl complex **1c** was prepared from the same precursor by reacting it with BzMgCl Grignard reagent [8].

Acetonitril was distilled and purified by standard methods and stored under argon. All reactions were carried out under argon using standard Schlenk techniques.

The ^{31}P and ^{1}H NMR spectra were taken on a Varian Inova 400 spectrometer operating at 400.13 MHz (^{1}H) and 161.89 MHz (^{31}P). Chemical shifts are reported in ppm relative to 85% H_3PO_4 or TMS (downfield) for ^{31}P and ^{1}H NMR, respectively. Elemental analyses were measured on a 1108 Carlo Erba apparatus.

*3.1.1. Synthesis of Pt{(S,S)-bdpp}(Me)$_2$ (**2a**) complex*

To a degassed solution of 66.7 mg (0.2 mmol) Pt(cod)(Me)$_2$ in 4 ml benzene a degassed solution of 88.1 mg (0.2 mmol) bdpp in 2 ml benzene is added under argon. The reaction mixture is stirred at room temperature for 16 h. Half of the solvent was distilled off and a white precipitate was formed. It was washed with hexane and dried in vacuum.

Yield: 60%. Anal. Calc. for $C_{31}H_{36}P_2Pt$ (665.65): C, 55.92; H, 5.45. Found: C, 56.11; H, 5.67%. For NMR see Table 1.

*3.1.2. Synthesis of Pt{(S,S)-bdpp}(Ph)$_2$ (**2b**) complex*

A procedure similar to that described for **2a** has been used.

Yield: 77%. Anal. Calc. for $C_{41}H_{40}P_2Pt$ (789.80): C, 62.35; H, 5.10. Found: C, 62.21; H, 5.40%. For NMR see Table 1.

*3.1.3. Synthesis of Pt{(S,S)-bdpp}(Bz)$_2$ (**2c**) complex*

A procedure similar to that described for **2a** has been used.

Yield: 58%. Anal. Calc. for $C_{43}H_{44}P_2Pt$ (817.85): C, 63.15; H, 5.42. Found: C, 63.30; H, 5.66%. For NMR see Table 1.

*3.1.4. Synthesis of Pt{(S,S)-bdpp}(2-Tioph)$_2$ (**2d**) complex*

A procedure similar to that described for **2a** has been used.

Yield: 79%. Anal. Calc. for $C_{37}H_{36}P_2PtS_2$ (801.84): C, 55.42; H, 4.53; S, 8.00. Found: C, 55.29; H, 4.65; S, 8.36%. For NMR see Table 1.

*3.1.5. Synthesis of Pt{(S,S)-bdpp}(Me)I (**3a**) complex*

13.3 mg (0.02 mmol) **2a** was suspended in 0.5 ml acetonitrile and 28.4 mg (0.2 mmol) methyl-iodide was added. It was stirred at 75 °C for 24 h (until the complex dissolved completely). The solvent was distilled off until yellow crystals of Pt{(*S*,*S*)-bdpp}(Me)I appeared.

Yield: 70%. Anal. Calc. for $C_{30}H_{33}P_2PtI$ (777.52): C, 46.34; H, 4.28. Found: C, 46.22; H, 4.39%. For NMR see Table 1.

*3.1.6. Synthesis of Pt{(S,S)-bdpp}(Ph)I (**3b**) complex*

To a solution of 167 mg (0.3 mmol) Pt(cod)I_2 in 13 ml dichloromethane 165.2 mg (0.45 mmol) $PhSnBu_3$ was added. It was refluxed under argon for 3 days. The solution was evaporated to dryness and the solid was washed with cold hexane (3 × 1 ml). The Pt(cod)(Ph)I was obtained as a grey powder-like material which has to be stored in a dark ampulle under argon or transferred immediately to a phosphine complex. Yield: 63%.

50.7 mg (0.1 mmol) Pt(cod)(Ph)I and 41.8 mg (0.095 mmol) (*S*,*S*)-bdpp was dissolved in 3 ml of dichloromethane and was stirred under argon for 14 h. The solvent was removed in vacuum and the white solid was washed with hexane and dried in vacuum.

Yield: 83%. Anal. Calc. for $C_{35}H_{35}P_2PtI$ (839.59): C, 50.07; H, 4.20. Found: C, 50.23; H, 4.36%. For NMR see Table 1.

*3.1.7. Synthesis of Pt{(S,S)-bdpp}(2-Tioph)I (**3d**) complex*

46.9 mg (0.1 mmol) Pt(cod)(2-Tioph)$_2$ and 44.6 mg (0.08 mmol) Pt(cod)I_2 was dissolved in 10 ml dichloromethane and stirred for two days at room temperature. The solvent was evaporated in vacuum and the Pt(cod)(2-Tioph)I was obtained as dark-yellow material.

51.3 mg (0.1 mmol) Pt(cod)(2-Tioph)I and 41.8 mg (0.095 mmol) (*S*,*S*)-bdpp was dissolved in 3 ml of dichloromethane and was stirred under argon for 14 h. The solvent was removed in vacuum and the yellow solid was washed with hexane and dried in vacuum.

Yield: 86%. Anal. Calc. for $C_{33}H_{33}P_2PtIS$ (845.62): C, 46.87; H, 3.93; S, 3.79. Found: C, 46.91; H, 4.06%. For NMR see Table 1.

*3.1.8. Synthesis of Pt{(S,S)-bdpp}I_2 (**4**) complex*

A synthetic procedure for **4** by using the conventional 'benzonitrile route' (reacting Pt(PhCN)$_2I_2$ with bdpp) has already been published [6]. An alternative method based on the ligand exchange reaction of the dimethyl complex **2a** can be used as follows.

13.3 mg (0.02 mmol) **2a** was suspended in 0.5 ml dry acetonitrile under argon. 26.8 mg (0.2 mmol) methylene iodide was added and kept at 80 °C for 2 h. A bright yellow homogeneous solution was obtained. The highly pure crystalline of Pt{(*S*,*S*)-bdpp}I_2 has been obtained upon cooling at 4 °C. All the analytical details (NMR, analysis) were identical with those published earlier for the same compound [6]. Yield: 60%.

3.1.9. X-ray crystal structure determination of [Pt{(S,S)-bdpp}I_2] · 1/3MeCN · 1/3CH_2I_2 and of [Pt{(S,S)-bdpp}(Me)I]

Crystals were mounted on a glass fiber in air and collected at room temperature, on a Bruker APEX CCD area-detector diffractometer for **4** and a Bruker SMART CCD for **3a**. Crystal data are reported in Table 4. Graphite-monochromatized Mo Kα ($\lambda = 0.71073$ Å) radiation was used with the generator working at 45 kV and 40 mA. Orientation matrixes were initially obtained from least-squares refinement on ca. 300 reflections measured in three different ω regions, in the range $0 < \theta < 23°$; cell parameters were optimized on the position, determined

Table 4
Crystal data and data collection parameters

Identification code	[Pt{(*S*,*S*)-bdpp}I_2] · 1/3 MeCN · 1/3 CH_2I_2 (**4**)	[Pt{(*S*,*S*)-bdpp}-(Me)I] (**3a**)
Empirical formula	$C_{30}H_{31.67}I_{2.67}N_{0.33}P_2Pt$	$C_{30}H_{33}IP_2Pt$
Formula weight	992.32	777.49
Temperature (K)	293(2)	293(2)
Wavelength (Å)	0.71069	0.71069
Crystal system, space group	$P2_1$	$P2_1$
Unit cell dimensions		
a (Å)	11.316(5)	11.1302(10)
b (Å)	14.305(5)	14.5032(13)
c (Å)	29.717(5)	18.6585(16)
β (°)	100.381(5)	106.229(2)
Volume (Å^3)	4732(3)	2891.9(4)
Z, calculated density (Mg/m^3)	6, 2.089	4, 1.786
Absorption coefficient (mm^{-1})	7.178	6.047
F(000)	2780	1496
Crystal size (mm)	0.3 × 0.2 × 0.1	0.2 × 0.15 × 0.1
θ Range for data collection (°)	0.70 to 31.38	1.81 to 32.76
Limiting indices	$-15 \leqslant h \leqslant 15$, $-20 \leqslant k \leqslant 20$, $-43 \leqslant l \leqslant 43$	$-16 \leqslant h \leqslant 16$, $-21 \leqslant k \leqslant 21$, $-28 \leqslant l \leqslant 27$
Reflections collected/unique	76998/28580 [$R_{int} = 0.0391$]	52539/19671 [$R_{int} = 0.0286$]
Completeness to $\theta = 31°$	94.3%	94.2%
Absorption correction	None	None
Refinement method	Full-matrix least-squares on F^2	Full-matrix least-squares on F^2
Data/restraints/parameters	28580/3/981	19671/1/619
Goodness-of-fit on F^2	1.023	0.999
Final R indices [$I > 2\sigma(I)$]	$R_1 = 0.0371$, $wR_2 = 0.0796$	$R_1 = 0.0288$, $wR_2 = 0.0685$
R indices (all data)	$R_1 = 0.0530$, $wR_2 = 0.0857$	$R_1 = 0.0427$, $wR_2 = 0.0738$
Absolute structure parameter	−0.010(2)	−0.001(3)
Largest difference in peak and hole (e A^{-3})	1.375 and −1.357	1.821 and −1.103

after integration, of ca. 8000 reflections. The intensity data were collected within the limits $2\theta < 62.8°$ (**4**) and $2\theta < 65.5°$ (**3a**) in the full sphere (ω scan method), with sample-detector distance fixed at 4.72 and 3.86 cm., respectively; 2400 frames (20 s per frame; $\Delta\omega = 0.3°$) were collected for both crystals; an empirical absorption correction was applied (SADABS [11]). The structures were solved by direct methods (SIR97 [12]) and refined with full-matrix least-squares (SHELX97 [13]) on the basis of 28,580 and 19,671 independent reflections, respectively; anisotropic temperature factors were assigned to all non-hydrogen atoms. Hydrogens were riding on their carbon atoms. The absolute configuration was determined by internal comparison and subsequently confirmed by the refined Flack parameter.

Crystallographic data for the structural analysis has been deposited with the Cambridge Crystallographic Data Centre, CCDC No. 287350 for compound **3a** and CCDC No. 287351 for compound **4**.

Acknowledgements

The authors thank the Hungarian Research Fund (TS044800) for the financial support.

References

[1] C.D. Frohning, C.W. Kohlpainter, in: B. Cornils, W.A. Herrmann (Eds.), Applied Homogeneous Catalysis with Organometallic Compounds, vol. 1, VCH, Weinheim, 1996, p. 29 ff;
I. Ojima, C.-Y. Tsai, M. Tzamarioudaki, D. Bonafoux, The Hydroformylation Reaction, in: L. Overman et al. (Eds.), Organic Reactions, Wiley, New York, 2000, pp. 1–354.
[2] S. Gladiali, J.C. Bayón, C. Claver, Tetrahedron: Asymmetry 6 (1996) 1453;
F. Agbossou, J.-F. Carpentier, A. Mortreux, Chem. Rev. 95 (1995) 2485.
[3] K.G. Anderson, R.J. Cross, Acc. Chem. Res. 17 (1984) 67;
M. Gómez, G. Muller, D. Sainz, J. Sales, Organometallics 10 (1991) 4036.
[4] I. Tóth, T. Kégl, C.J. Elsevier, L. Kollár, Inorg. Chem. 33 (1994) 5708;
T. Kégl, L. Kollár, L. Radics, Inorg. Chim. Acta 265 (1997) 249.
[5] G. Consiglio, P. Pino, L.I. Flowers, C.U. Pittmann Jr., J. Chem. Soc., Chem. Commun. (1983) 612;
P. Haelg, G. Consiglio, P. Pino, J. Organomet. Chem. 296 (1985) 281;
G. Consiglio, F. Morandini, M. Scalone, P. Pino, J. Organomet. Chem. 279 (1985) 193;
L. Kollár, G. Consiglio, P. Pino, J. Organomet. Chem. 330 (1987) 305;
L. Kollár, J. Bakos, I. Tóth, B. Heil, J. Organomet. Chem. 370 (1989) 257;
G. Consiglio, S.C.A. Nefkens, A. Borer, Organometallics 10 (1991) 2046;
I. Tóth, I. Guo, B. Hanson, Organometallics 12 (1993) 848;
G. Parrinello, J.K. Stille, J. Am. Chem. Soc. 109 (1987) 7122.
[6] E. Farkas, L. Kollár, M. Moret, A. Sironi, Organometallics 15 (1996) 1345.
[7] C. Eaborn, K.J. Odell, A. Pidcock, J.C.S. Dalton (1978) 357.
[8] H.C. Clark, L.E. Manzer, J. Organomet. Chem. 59 (1973) 411.
[9] The fact that δ-skew conformations have a smaller 'bite' angle than the other ones can be also verified in the crystal structure determinations of [Rh(BDPP)(NBD)]$^+$ [(chair) P-Rh–P 95.1(3)°] and [Rh(BDPP)(COD)]$^+$ [(δ-skew) P-Rh–P 88.6(1)°] J. Bakos, I. Tóth, B. Heil, G. Szalontai, L. Párkányi, V. Fülöp, J. Organomet. Chem. 370 (1989) 263.
[10] H.B. Bürgi, J.D. Dunitz, Acc. Chem. Res. 16 (1983) 153.
[11] G.M. Sheldrick, SADABS, University of Göttingen, Germany, 1996.
[12] A. Altomare, M.C. Burla, M. Camalli, G.L. Cascarano, C. Giacovazzo, A. Guagliardi, A.G.G. Moliterni, G. Polidori, R. Spagna, J. Appl. Cryst. 32 (1999) 115–119.
[13] G.M. Sheldrick, Programs for Crystal Structure Analysis (Release 97-2), Institut für Anorganische Chemie der Universität, Tammannstrasse4, D-3400 Göttingen, Germany, 1998.
[14] J.L. Portscheller, S.E. Lilly, H.C. Malinakova, Organometallics 22 (2003) 2961.
[15] I. Tóth, C.J. Elsevier, J.D. De Vries, J. Bakos, W.J.J. Smeets, A.L. Spek, J. Organomet. Chem. 540 (1997) 15.